Early apple bruise recognition based on near-infrared imaging and grayscale gradient images

Zengrong Yang
China Agricultural University
Yuhui Yuan
China Agricultural University
Jianhua Zheng
China Agricultural University
Huaibin Wang
China Agricultural University
Junhui Li
China Agricultural University
Longlian Zhao (zsczll@cau.edu.cn)
China Agricultural University

Research Article

Keywords: Apple, Early bruise, Near-infrared imaging, Gradient grayscale image, Edge recognition

Posted Date: June 22nd, 2022

DOI: https://doi.org/10.21203/rs.3.rs-1757799/v1

Abstract

Early apple bruises, especially those occurring within half an hour, usually have no external symptoms and are difficult to find. In this study, a fast and nondestructive detection method for early bruises based on a near-infrared camera and image recognition was developed. A total of thirty apple samples were photographed on both sides of each apple. Grayscale images of the apples were captured using a near-infrared camera with a wavelength region between 900 and 2350 nm. Images of apples (n = 62) without bruises were collected. The same apples were artificially damaged and photographed by the near-infrared camera immediately. The apples were photographed again at 30–35 min after bruising, and a total of 186 grayscale images were collected. As the glossiness of apples limits the accuracy in the detection of defects, a compound method was proposed consisting of nonlinear grayscale transformation and frequency-domain image filtering techniques, followed by the first derivative to obtain the gradient grayscale image. Since bruises had distinct edges, bruise edge pixels were detected instead of sound bruise pixels. The compound method obtained a 97.62% classification accuracy for nonbruised apples and apples with fresh bruises. The experimental results show that it is feasible to identify early bruises in apples based on near-infrared camera imaging and gradient grayscale images. The method can also provide a reference for the in-situ nondestructive early bruise detection of apples and other fruits.

1. Introduction

Apple defects can be divided into four main categories: mechanical damage, pathological disorders, contamination, and physiological disorders. These defects reduce the quality of apples, affect the sales price, and may be harmful to human health (Zhu et al., 2016; Lu and Lu, 2017). Apple bruises are typical mechanical damage that can easily occur during picking, sorting, packaging, and transportation (Van Zeebroeck et al., 2006; Xing et al., 2005). Identifying and classifying bruised apples as early as possible is conducive to the storage and circulation of apples. It can also prevent decaying and deteriorating apples from affecting other healthy apples (Zhang et al., 2017). Severe bruises can be identified with the naked eye or machine vision technology. However, early mild apple bruises, especially those occurring within half an hour, usually have no obvious external symptoms and are difficult to find (Keresztes et al., 2016; Lu et al., 2016). Therefore, it is necessary to find a fast, accurate, convenient and nondestructive discrimination method for apples with early bruises.

When the surface of an apple suffers mechanical damage, such as bumps, the pulp tissue is destroyed. The physiological metabolism of the damaged part will be disordered over time, the release of ethylene will increase, the respiratory strength will increase significantly, and the soluble solid content will be relatively reduced (Agar et al., 1999; Watada et al., 1996). In the initial stage of the bruises, under visible light, there is no obvious difference between the appearance of the bruised area and the healthy area; thus, a detection method based on visible light is subject to certain restrictions in this case. Due to the complex background and large discrepancies in the surface color, slight and early bruises are difficult to distinguish by image processing technology under visible light (Pan et al., 2019; Xing and De Baerdemaeker, 2007). The penetrability of near-infrared light in a tissue sample is deeper than that of

visible light (Ding et al., 2021), and it is quite sensitive to changes in water content and soluble solids in the sample (Li et al., 2019; Takano et al., 2020). Therefore, a near-infrared image of an apple can more easily reveal bruising than a visible light image, which makes it possible for near-infrared imaging to identify early bruises in apples. Methods based on near-infrared imaging, including hyperspectral imaging and near-infrared camera imaging, have developed rapidly in recent years and are appropriate for the nondestructive detection of early bruises in apples.

Hyperspectral imaging technology integrates imaging, spectroscopy, chemometrics, and other optical sensing technologies. It is a nondestructive, noncontact detection technology that allows the simultaneous acquisition of sample spatial and spectral information (Xing and De Baerdemaeker, 2005; Al-Sarayreh et al., 2020). In recent years, hyperspectral imaging technology has been widely used to identify defects in various fruits, including the detection of early apple bruises (Lu et al., 2020). For example, Tan et al. (2018) used hyperspectral imaging combined with principal component analysis to identify early bruises in apples with a recognition rate of 99.9%. Luo et al. (2019) used hyperspectral and multispectral reflectance imaging technology to identify apple bruises within one hour, and the recognition rate reached 99.2%. Compared with other technologies, hyperspectral imaging technology not only reflects external characteristics such as the texture and size of the measured object but also reflects internal quality information such as the chemical composition content of the object (Lee et al., 2014). Since the information includes the spectral signature and the figure (Baranowski et al., 2013) is sufficient, hyperspectral imaging technology usually has a higher recognition rate. However, the three-dimensional data cube in this method has considerable redundant information, which increases the complexity of data processing (Du et al., 2017; Sui et al., 2015). Additionally, the calibration models are usually not independent of the particular calibration samples, measurement technique, or the setup of specific experiments.

Near-infrared camera imaging technology for identifying apple bruises is simple, fast, and highly sensitive. Near-infrared cameras have the advantages of small size, light weight, high luminous flux, and convenient data collection (Ge et al., 2016; Zhang et al., 2021). In conclusion, near-infrared imaging technology is suitable for the nondestructive detection of apple bruises. Aleixos et al. (2002) developed an imaging system based on a multispectral camera that can obtain visible light and near-infrared images from the same scene. The system can detect the size, color, and presence of defects in citrus and can also correctly classify lemons and citrus. Kleynen et al. (2003) proposed a method based on quadratic discriminant analysis that selects the best filter wavelength and constructs a multispectral imaging system to detect multiple defects in "Jonagold" apples. The combination of filters with three different wavelengths is sufficient to detect most bruised apples, and the combination of filters with four different center wavelengths has a classification accuracy of 100% for apples with severe defects and moderate defects. A near-infrared camera developed with T2SL material has a smaller dark current, lower noise, and higher sensitivity. It offers great target recognition and detailed expression under environmental conditions such as night vision and low visibility. For this reason, this study used a T2SL near-infrared camera with a wavelength range of 900–2350 nm to collect near-infrared images of bruised apple samples. A recognition method of apple bruises for detecting bruise edges was proposed, which

could realize the nondestructive detection of early bruises (within half an hour) on apples. Bruised apples have lower reflectance than nonbruised apples in the visible light region, especially in the near-infrared light region. Thus, near-infrared images are more suitable for detecting bruises than visible light images.

2. Materials And Methods

2.1 Samples and bruise manufacturing device

As one of the major varieties of apples, Red Fuji apples have a wider peel variation than other apple varieties. Thus, it is harder to detect early bruises on Red Fuji apples. Therefore, apple bruise recognition experiments using Red Fuji apples are more representative. In this experiment, 31 Red Fuji apples from Yantai Qixia were used as the research object. Since the difference in position 180° apart along the horizontal line was even greater than that of different apples, the relative position of every apple was photographed separately, and the sample set can be regarded as 62. Before the experiment, the apples were placed at room temperature for twelve hours, and the surfaces of the apples were disinfected with 75% alcohol.

The purpose of this study is to detect bruised apples that are damaged within half an hour. Early bruises can only be artificially created because fresh bruises cannot be distinguished by the naked eye. The device for making bruises is a pendulum with a diameter of 18 mm and a weight of 0.085 kg. The pendulum is placed at one end of a pendulum rod with a length of 0.4 m. A schematic diagram is shown in Fig. 1. The pendulum is raised to an angle of 45° with the vertical direction and released to make the pendulum impact fixed apples. The bruised area is small and approximately 0.8 cm^2. Commonly, the apple surface is intact and has a slight depression that is not easily recognized by the naked eye (Stropek and Gołacki, 2013; Diels et al., 2017).

2.2 Near-infrared camera imaging system

The apple images were collected with a near-infrared camera (Xeva-2.35-320, Xenics, Belgium), which uses a thermoelectrically cooled T2SL detector with a 320×256 pixel resolution and a 900–2350 nm wavelength response. The camera lens is from the KOWA Group of Japan Kowa Co., Ltd., which has manual focus and aperture functions. The maximum aperture is F1.4.

The system consists of a near-infrared camera, a tripod, and three halogen tungsten lamps, as shown in Fig. 2. The near-infrared camera is fixed by a tripod, and the lens is vertically downward to the apple. As the apple has an irregular spherical shape and the camera has no light source, three tungsten halogen lamps are added to minimize the impact of uneven illumination while collecting images. The three lamps are placed at an angle of 120° with the apple sample as the center. The angle between the irradiation direction and the vertical direction is approximately 45°, and the lampshade is wrapped with a soft cloth to make the light more uniform.

Images were collected by the built-up system, and near-infrared images (n = 62) of nonbruised apples were collected first. Then, the device shown in Fig. 1 was used to create apple bruises, and near-infrared images (n = 62) of the apples were acquired immediately after the bruise appeared. Near-infrared images (n = 62) of the same bruised apples were collected again 30 min later.

Compared with visible light, near-infrared light is more sensitive to changes in organic components in apple samples. Therefore, near-infrared images of apples can more easily reveal bruises in the early stage of bruises than visible light images. In most cases, it is difficult to distinguish bruises with the naked eye in the visible light images of apples bruised for less than 30 min. We used a mobile phone to take an image of the apple immediately after the bruise occurred, as shown in Fig. 3(a). At the same time, a near-infrared image of the same apple was taken using a near-infrared camera, shown in Fig. 3(b). The location of the bruise in the apple is visible in the near-infrared image; however, the location of the bruise in the visible light image cannot be found.

2.3 Image processing method for early apple bruise recognition

This paper presents an image processing method for the detection of bruised apples. The compound method contains two-level image preprocessing, including nonlinear grayscale transformation and frequency-domain image filtering. To eliminate the interference of background information on the target apple image and extract the region of interest, which is the fruit body, a mask is made in advance using the threshold segmentation method (Kang et al., 2009; Shirly and Ramesh, 2019). After background processing, the image is subjected to nonlinear gray transform, high-pass filtering and image derivation.

2.3.1 Nonlinear grayscale transformation

The gray value of the bruised part of the apple is lower than that of the nonbruised part, so the low gray areas in the apple image can be used to identify the bruises as they are detected. In the process of extracting the edge of the bruise, the change in gray value in the target area caused by uneven illumination will affect the identification and extraction of the bruises. For example, the light spot caused by the supplementary light source in the target image is the region with a high gray value in the image (Keresztes et al., 2017).The light spot would be easily recognized as a bruise when the edge recognition method was used to extract damage. Therefore, it is particularly important to eliminate light spots in the original apple image (Zhang et al., 2009). To solve this problem, a two-level image processing method was designed.

First, a piecewise-linear grayscale transformation was used to weaken the light spot with a high gray value.

The grayscale level transformation uses a transformation function to map the input pixel gray value $f(x, y)$to a new gray value $g(x, y)$, which belongs to an image enhancement technology, as in Formula (1).

$$g(x, y) = T[f(x, y)](1)$$

To reduce the gray value of the light spot without affecting the contrast of the low gray area, the average gray value $aver1$ of the apple image is calculated before the grayscale conversion. The average gray value was set as a threshold, the pixels with a gray value that was smaller than the average gray value remained constant, and the gray value greater than the average gray value was compressed. The grayscale transformation function is shown in Formula (2), and the value of $aver1$is calculated as Formula (3).

$$g(x, y) = \begin{cases} f(x, y)(0 \le f(x, y) \le \text{aver1}) \\ a * f(x, y)(\text{aver1} < f(x, y) \le 1)(0 < a < 1) \end{cases} (2)$$

$$aver1 = \frac{\sum_{i=1}^{n} f_i(x, y)}{n} (3)$$

Nonlinear transformations, such as logarithmic transformations, can increase the smoothness of image processing. The logarithmic transformation is expressed as follows.

$$h(x, y) = b * \ln[g(x, y) + 1](4)$$

The gray value of the apple image is adjusted to ensure that the average brightness of the transformed images of different apple samples remains consistent. The average gray value of $h(x, y)$ is set to be $aver3$, and the gray value of each pixel is h_i before adjustment. The average gray value of the apple image is $aver4$, and the gray value of each pixel is $h_i^{'}$ after adjustment. Formula (5) can be obtained.

$$h_i^{'} = h_i * \frac{aver4}{aver3} (5)$$

The above is the first level of image processing, and the contrast of the image is improved after the processing.

2.3.2 Frequency-domain image filtering

The image is further processed by a second-level processing method. A high-pass filter in the frequency domain is designed to further weaken the influence of uneven illumination and improve the contrast of the bruised area. First, a Fourier transform is performed on the image signal. In the frequency domain, the image signal can be regarded as composed of high-frequency components and low-frequency components. According to Retinex Theory, an apple's near-infrared image signal can also be regarded as composed of illumination components and diffuse reflection components (Land, 1986). The illumination component of the sample caused by uneven illumination corresponds to the low-frequency signal, and the diffuse reflection component corresponds to the high-frequency signal, which carries the main characteristic information of the sample. Therefore, a high-pass filtering method is selected as the second level of image preprocessing (Tseng and Lee, 2017; Adelmann, 1998).

The transfer function of the selected Butterworth filter is shown in Formula (6).

$$H(u, v) = \frac{1}{1 + \left[\frac{D_0}{D(u,v)} \right]^{2N}} (6)$$

After frequency-domain filtering, the bruise edge is more obvious, and the contrast of the image is improved, which is conducive to bruise identification and extraction.

2.3.3 Image derivation to obtain the gray gradient image

Due to the low grayscale region caused by bruises having a greater grayscale change ratio at the edge of the low grayscale region, a grayscale gradient image by the first derivative is acquired to manifest this character. Two images, including a horizontal grayscale gradient image and a vertical grayscale gradient image, are acquired by the first derivative. The absolute values of the two images are calculated and then added. Where the gray value of the original grayscale image has a small change ratio, the gray value of the corresponding position in the grayscale gradient image will be close to zero. In contrast, the gray value of the corresponding position in the grayscale gradient image deviates from zero. The greater the rate of change in the original image gray value, the greater the gray value of the corresponding position in the gradient grayscale image. Then, threshold segmentation is used to binarize the gradient image, which can well express the edge characteristics of the gradient grayscale image. In the process of identifying the edge of the bruised area, it is necessary to exclude the influence of the profile of the apple. In the background processing process, the binarized image of the original grayscale image is obtained, which is a mask. The corrosion-treated mask is multiplied by the new binarized image to eliminate the entire edge of the apple, and then the binary image only shows the edges of the bruise. Counting the number of pixels with a gray value of 1 can determine whether the image is an image of a bruised apple.

3. Results And Discussion

3.1 Results of image processing flow

A low gray area can appear in the apple image for two reasons: the apple tissue in the region is damaged, or the region cannot receive enough light while the apple image is collected. As the surface of the apple is not a regular spherical shape, some images of nonbruised apples have low gray areas after image preprocessing. Such sound apples would be classified as bruised apples easily using the threshold segmentation method directly, which is an important factor that lowers the recognition rate of the threshold segmentation method. Therefore, the image gradient is calculated as 2.3.3. The bruise edge calculation for an apple sample is shown in Fig. 4.

Every apple image was processed by nonlinear gray transform, high-pass filtering and derivation. Taking the image of a bruised apple as an example, the whole process is shown in Fig. 5. Figure 5(a) shows the original images, Fig. 5(b) shows the images after nonlinear grayscale transformation, Fig. 5(c) shows the

images after frequency-domain image filtering, and Fig. 5(d) shows the images after derivation. The location of bruises could be explained by binarization of the image, as shown in Fig. 5(e). Then, Fig. 5(f) can be obtained by further corrosion processing. The number of pixels with a pixel value of 1 is counted to determine whether the image is a bruised image.

3.2 Identification results

The filtered images were derived and binarized in turn. If it was an image of a bruised apple, only the outline of the apple could be seen. Figure 6 randomly lists the identification results of 20 sound apples in the test set, and all samples were correctly identified.

If there was an image of a bruised apple, the outline of the apple and the outline of the bruise were all visible. Image processing was performed on some bruised apple images in the test set, and the results are shown in Fig. 7. The samples of bruised apples were all correctly identified.

In image processing, there were two key parameters: one was the cutoff frequency of the frequency domain filter, and the other was the threshold for binarization after image derivation. The parameters were set by 20 images of sound apples and 40 images of bruised apples. The remaining 126 apple images, including 42 images of nonbruised apples and 84 images of bruised apples, were used to verify this method. The test results are shown in Table 1.

Table 1
Apple bruise recognition result based on the edge extraction method

The type of apples	Number of samples	Result of recognition		Accuracy (%)
		Sound	Bruised	
Sound	42	41	1	97.62
Bruised (0 min)	42	2	40	95.24
Bruised (30 min)	42	0	42	100.00

The image recognition method that is commonly used is threshold segmentation without derivation, and the threshold is determined according to the grayscale histogram. To compare with the method in this paper, all the images were preprocessed in the same way, and a threshold segmentation method was used to recognize the bruised region instead of extracting the bruised edge. The same 126 pictures were used for verification. The results are shown in Table 2.

Table 2
Apple bruise recognition result based on the threshold segmentation method

The type of apples	Number of samples	Result of recognition		Accuracy (%)
		Sound	Bruised	
Sound	42	37	5	88.10
Bruised (0 min)	42	2	40	95.24
Bruised (30 min)	42	2	40	95.24

The lossless apple image is marked as 0 and the damaged apple image is marked as 1. The binary classification confusion matrix of the method with derivation is shown in Fig. 8(a). The accuracy, precision and recall of the method are 97.6%, 98.8% and 97.6%, respectively. The binary classification confusion matrix of the method without derivation is shown in Fig. 8(b). The accuracy, precision and recall of the method are 92.9%, 94.1% and 95.2%, respectively. Therefore, using an image gradient to identify apple bruises can effectively improve the recognition rate.

3.3 Discussion

Detecting apple bruises by collecting near-infrared images and conducting image recognition is a simple and convenient method. Compared with hyperspectral imaging, this method only uses partial band information. By comparison, it is found that different image preprocessing methods affect the image recognition effect.

Threshold segmentation is commonly used for extracting the bruised region. Preprocessing is necessary before recognizing an apple image. It is impossible to eliminate the influence of uneven illumination during the pretreatment; thus, the misjudgment of sound apples is a common outcome. A low grayscale region in apple images will appear due to uneven illumination or bruises; however, the low gray areas caused by bruises usually have obvious edges. Therefore, it is more reasonable to identify the bruise edge pixels instead of the entire bruise pixels.

Image processing methods for identifying apple bruises do not involve establishing statistical models. These methods require a small number of samples to determine the key parameters of the algorithm. If the cutoff frequency is larger, there will be a more obvious filtering effect. The recognition rate of sound apples increases, while the recognition rate of bruised apples decreases. In contrast, if the filtering effect is weakened, the recognition rate of the sound apples decreases, and the recognition rate of bruised apples increases. If the cutoff frequency is variable, the bruise recognition result will be further improved.

4. Conclusions

In this study, a near-infrared camera was used to collect near-infrared images of sound apples and apples bruised within half an hour. A two-level image preprocessing method was used. Then, the edge of the

bruised area was extracted by the gradient grayscale image, which reflected the rate of change of the grayscale. The recognition accuracy of all apples was 97.62%. From the obtained gradient grayscale image, the location of the bruises in the apples could be seen clearly. Therefore, it is feasible to use near-infrared camera imaging technology and image processing methods to identify bruises on apples or other fruits. This study provides a reference method for the online or in vivo detection of apple bruises in the future.

Declarations

Acknowledgments

The research was supported by the National Natural Science Foundation of China (Grant No. 31172064).

Author Contributions Statement

Zengrong Yang developed the theory, performed the computations and wrote the manuscript with support from Jianhua Zheng and Junhui Li. Huaibin Wang and Yuhui Yuan carried out the experiment. Longlian Zhao investigated and supervised the findings of this work. All authors discussed the results and contributed to the final manuscript.

Data Availability Statement

Some or all data, models, or code generated or used during the study are available from the corresponding author by request. (List items).

Conflict of Interest Statement

We declare that we have no conflict of interest. The authors have no competing interests as defined by Springer, or other interests that might be perceived to influence the results and/or discussion reported in this paper.

References

1. Adelmann, H.G., 1998. Butterworth equations for homomorphic filtering of images. Comput. Biol. Med. 28 (2), 169–181. https://doi.org/10.1016/s0010-4825(98)00004-3.
2. Agar, I.T., Massantini, R., Hess-Pierce, B., Kader, A.A., 1999. Postharvest co2 and ethylene production and quality maintenance of fresh-cut kiwifruit slices. J. Food Sci. 64 (3), 433–440. https://doi.org/10.1111/j.1365-2621.1999.tb15058.x.
3. Aleixos, N., Blasco, J., Navarrón, F., Moltó, E., 2002. Multispectral inspection of citrus in real-time using machine vision and digital signal processors. Comput. Electron. Agr. 33 (2), 121–137. https://doi.org/10.1016/S0168-1699(02)00002-9.

4. Al-Sarayreh, M., Reis, M.M., Yan, W.Q., Klette, R., 2020. Potential of deep learning and snapshot hyperspectral imaging for classification of species in meat. Food Control 117, 107332. https://doi.org/10.1016/j.foodcont.2020.107332.
5. Baranowski, P., Mazurek, W., Pastuszka-Woźniak, J., 2013. Supervised classification of bruised apples with respect to the time after bruising on the basis of hyperspectral imaging data. Postharvest Biol. Tec. 86, 249–258. https://doi.org/10.1016/j.postharvbio.2013.07.005.
6. Diels, E., van Dael, M., Keresztes, J., Vanmaercke, S., Verboven, P., Nicolai, B., Saeys, W., Ramon, H., Smeets, B., 2017. Assessment of bruise volumes in apples using x-ray computed tomography. Postharvest Biol. Tec. 128, 24–32. https://doi.org/10.1016/j.postharvbio.2017.01.013.
7. Ding, C., Huang, Y., Shen, Z., Chen, X., 2021. Synthesis and bioapplications of ag2 s quantum dots with near-infrared fluorescence. Adv. Mater. 33 (32), 2007768. https://doi.org/10.1002/adma.202007768.
8. Du, B., Zhang, M., Zhang, L., Hu, R., Tao, D., 2017. Pltd: patch-based low-rank tensor decomposition for hyperspectral images. IEEE T. Multimedia 19 (1), 67–79. https://doi.org/10.1109/TMM.2016.2608780.
9. Ge, Y., Bai, G., Stoerger, V., Schnable, J.C., 2016. Temporal dynamics of maize plant growth, water use, and leaf water content using automated high throughput rgb and hyperspectral imaging. Comput. Electron. Agr. 127, 625–632. https://doi.org/10.1016/j.compag.2016.07.028.
10. Kang, W., Yang, Q., Liang, R., 2009. The comparative research on image segmentation algorithms (Vol. 2, pp. 703–707): IEEE.
11. Keresztes, J.C., Diels, E., Goodarzi, M., Nguyen-Do-Trong, N., Goos, P., Nicolai, B., Saeys, W., 2017. Glare based apple sorting and iterative algorithm for bruise region detection using shortwave infrared hyperspectral imaging. Postharvest Biol. Tec. 130, 103–115. https://doi.org/10.1016/j.postharvbio.2017.04.005.
12. Keresztes, J.C., Goodarzi, M., Saeys, W., 2016. Real-time pixel based early apple bruise detection using short wave infrared hyperspectral imaging in combination with calibration and glare correction techniques. Food Control 66, 215–226. https://doi.org/10.1016/j.foodcont.2016.02.007.
13. Kleynen, O., Leemans, V., Destain, M.F., 2003. Selection of the most efficient wavelength bands for 'jonagold' apple sorting. Postharvest Biol. Tec. 30 (3), 221–232. https://doi.org/10.1016/S0925-5214(03)00112-1.
14. Land, E.H., 1986. An alternative technique for the computation of the designator in the retinex theory of color vision. Proceedings of the National Academy of Sciences - PNAS 83 (10), 3078–3080. https://doi.org/10.1073/pnas.83.10.3078.
15. Lee, W., Kim, M.S., Lee, H., Delwiche, S.R., Bae, H., Kim, D., Cho, B., 2014. Hyperspectral near-infrared imaging for the detection of physical damages of pear. J. Food Eng. 130, 1–7. https://doi.org/10.1016/j.jfoodeng.2013.12.032.
16. Li, Z., Zhou, X., Yang, J., Fu, B., Zhang, Z., 2019. Near-infrared-responsive photoelectrochemical aptasensing platform based on plasmonic nanoparticle-decorated two-dimensional photonic

crystals. ACS Appl. Mater. Inter. 11 (24), 21417–21423. https://doi.org/10.1021/acsami.9b07128.

17. Lu, Y., Li, R., Lu, R., 2016. Structured-illumination reflectance imaging (siri) for enhanced detection of fresh bruises in apples. Postharvest Biol. Tec. 117, 89–93. https://doi.org/10.1016/j.postharvbio.2016.02.005.
18. Lu, Y., Lu, R., 2017. Non-destructive defect detection of apples by spectroscopic and imaging technologies: a review. T. ASABE 60 (5), 1765–1790. https://doi.org/10.13031/trans.12431.
19. Lu, Y., Saeys, W., Kim, M., Peng, Y., Lu, R., 2020. Hyperspectral imaging technology for quality and safety evaluation of horticultural products: a review and celebration of the past 20-year progress. Postharvest Biol. Tec. 170, 111318. https://doi.org/10.1016/j.postharvbio.2020.111318.
20. Luo, W., Zhang, H., Liu, X., 2019. Hyperspectral/multispectral reflectance imaging combining with watershed segmentation algorithm for detection of early bruises on apples with different peel colors. Food Anal. Method. 12 (5), 1218–1228. https://doi.org/10.1007/s12161-019-01456-0.
21. Pan, X., Sun, L., Li, Y., Che, W., Ji, Y., Li, J., Li, J., Xie, X., Xu, Y., 2019. Non-destructive classification of apple bruising time based on visible and near-infrared hyperspectral imaging. J. Sci. Food Agr. 99 (4), 1709–1718. https://doi.org/10.1002/jsfa.9360.
22. Shirly, S., Ramesh, K., 2019. Review on 2d and 3d mri image segmentation techniques. Curr. Med. Imaging Rev. 15 (2), 150–160. https://doi.org/10.2174/1573405613666171123160609.
23. Stropek, Z., Gołacki, K., 2013. The effect of drop height on bruising of selected apple varieties. Postharvest Biol. Tec. 85, 167–172. https://doi.org/10.1016/j.postharvbio.2013.06.002.
24. Sui, C., Tian, Y., Xu, Y., Xie, Y., 2015. Unsupervised band selection by integrating the overall accuracy and redundancy. IEEE Geosci. Remote S. 12 (1), 185–189. https://doi.org/10.1109/LGRS.2014.2331674.
25. Takano, Y., Miyake, K., Sobhanan, J., Biju, V., Tkachenko, N.V., Imahori, H., 2020. Near-infrared light control of membrane potential by an electron donor–acceptor linked molecule. Chem. Commun. 56 (83), 12562–12565. https://doi.org/10.1039/D0CC05326K.
26. Tan, W., Sun, L., Yang, F., Che, W., Ye, D., Zhang, D., Zou, B., 2018. The feasibility of early detection and grading of apple bruises using hyperspectral imaging. J. Chemometr. 32 (10), e3067. https://doi.org/10.1002/cem.3067.
27. Tseng, C., Lee, S., 2017. Closed-form designs of digital fractional order butterworth filters using discrete transforms. Signal Process. 137, 80–97. https://doi.org/https://doi.org/10.1016/j.sigpro.2017.01.015.
28. Van Zeebroeck, M., Tijskens, E., Dintwa, E., Kafashan, J., Loodts, J., De Baerdemaeker, J., Ramon, H., 2006. The discrete element method (dem) to simulate fruit impact damage during transport and handling: model building and validation of dem to predict bruise damage of apples. Postharvest Biol. Tec. 41 (1), 85–91. https://doi.org/10.1016/j.postharvbio.2006.02.007.
29. Watada, A.E., Ko, N.P., Minott, D.A., 1996. Factors affecting quality of fresh-cut horticultural products. Postharvest Biol. Tec. 9 (2), 115–125. https://doi.org/https://doi.org/10.1016/S0925-5214(96)00041-5.

30. Xing, J., De Baerdemaeker, J., 2005. Bruise detection on ‘jonagold’ apples using hyperspectral imaging. Postharvest Biol. Tec. 37 (2), 152–162. https://doi.org/10.1016/j.postharvbio.2005.02.015.
31. Xing, J., De Baerdemaeker, J., 2007. Fresh bruise detection by predicting softening index of apple tissue using vis/nir spectroscopy. Postharvest Biol. Tec. 45 (2), 176–183. https://doi.org/10.1016/j.postharvbio.2007.03.002.
32. Xing, J., Van Linden, V., Vanzeebroeck, M., De Baerdemaeker, J., 2005. Bruise detection on jonagold apples by visible and near-infrared spectroscopy. Food Control 16 (4), 357–361. https://doi.org/10.1016/j.foodcont.2004.03.016.
33. Zhang, J., Yang, G., Xu, Q., Zhao, Y., 2009. Adaptive calculation of division points for piecewise linear transformation and application in image enhancement (Vol. 1, pp. 645–648): IEEE.
34. Zhang, N., Li, P., Liu, H., Huang, T., Liu, H., Kong, Y., Dong, Z., Yuan, Y., Zhao, L., Li, J., 2021. Water and nitrogen in-situ imaging detection in live corn leaves using near-infrared camera and interference filter. Plant Methods 17 (1). https://doi.org/10.1186/s13007-021-00815-5.
35. Zhang, S., Wu, X., Zhang, S., Cheng, Q., Tan, Z., 2017. An effective method to inspect and classify the bruising degree of apples based on the optical properties. Postharvest Biol. Tec. 127, 44–52. https://doi.org/10.1016/j.postharvbio.2016.12.008.
36. Zhu, Q., Guan, J., Huang, M., Lu, R., Mendoza, F., 2016. Predicting bruise susceptibility of ‘golden delicious’ apples using hyperspectral scattering technique. Postharvest Biol. Tec. 114, 86–94. https://doi.org/10.1016/j.postharvbio.2015.12.007.

Figures

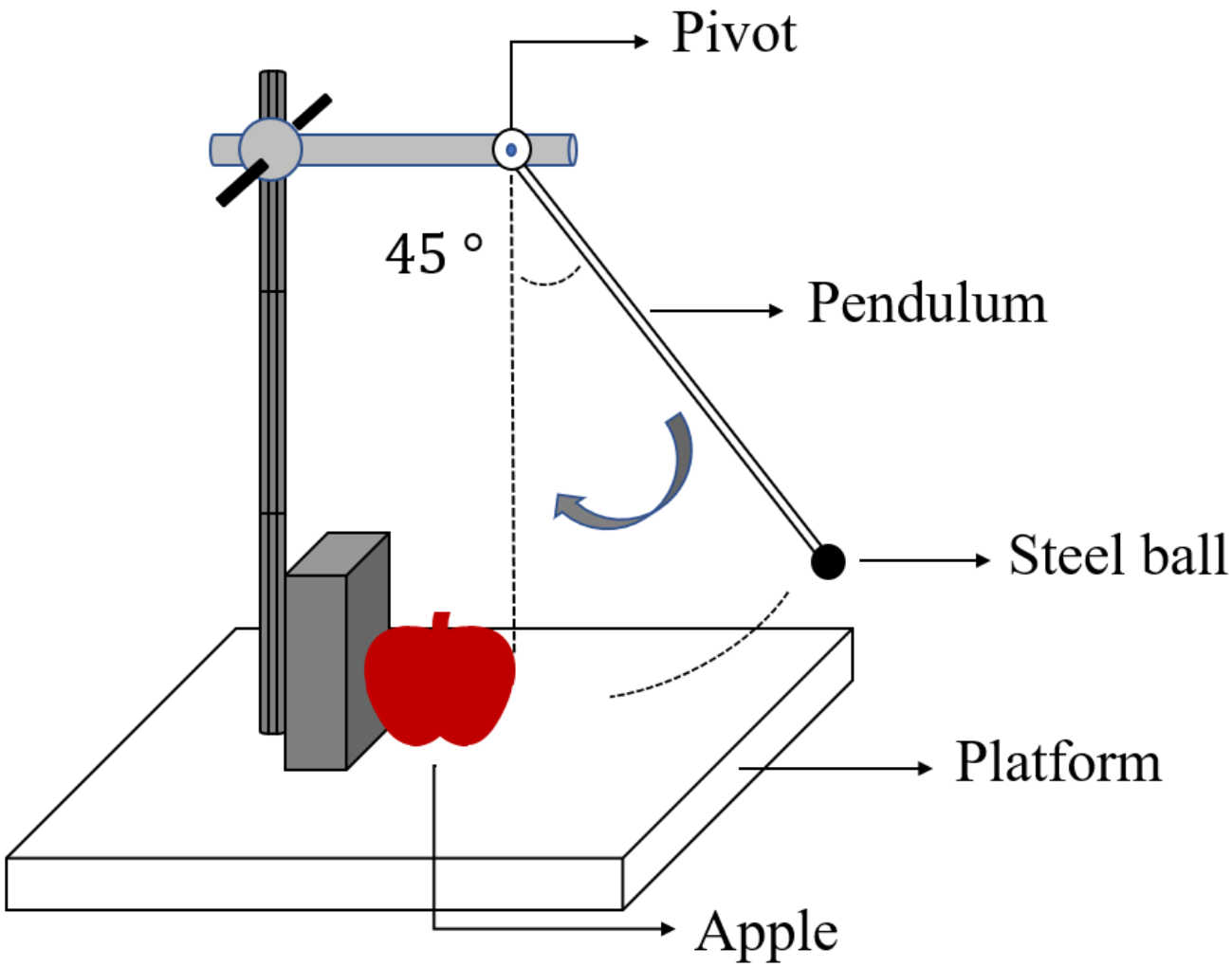

Figure 1

Schematic diagram of the device for manufacturing apple bruises

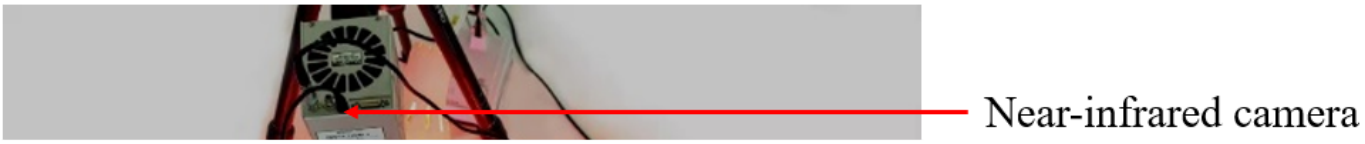

Figure 2

The system for acquisition of the near-infrared image

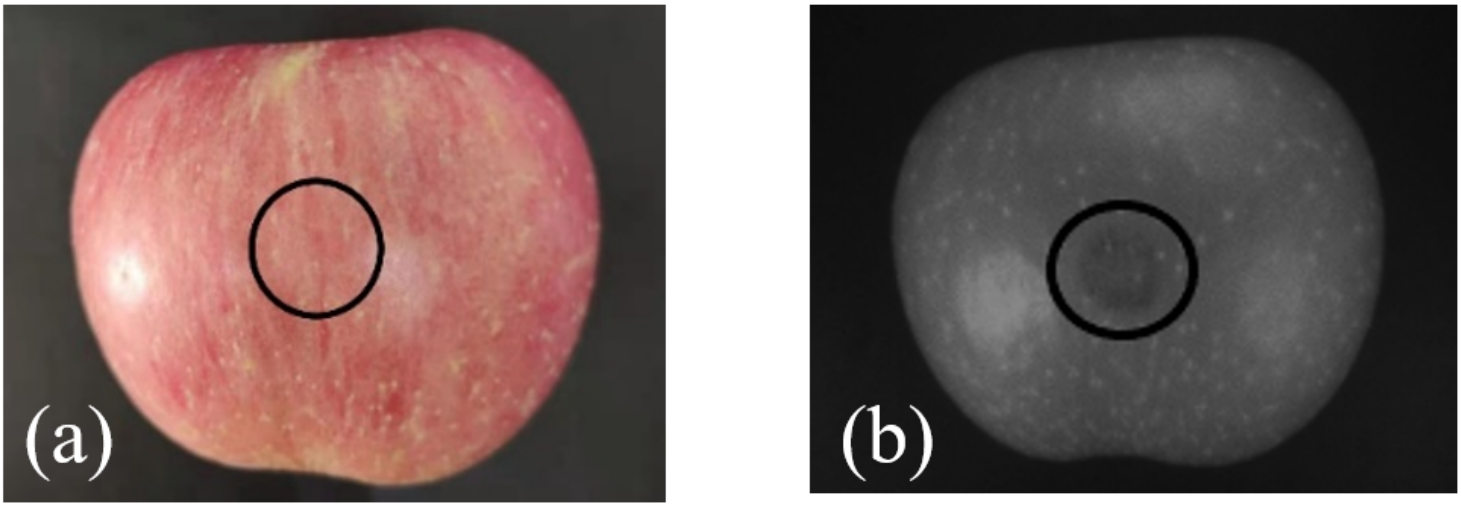

Figure 3

Comparison of visible light images and near-infrared images. (a) The visible-light image of a bruised apple. (b) Near-infrared image of the same bruised apple.

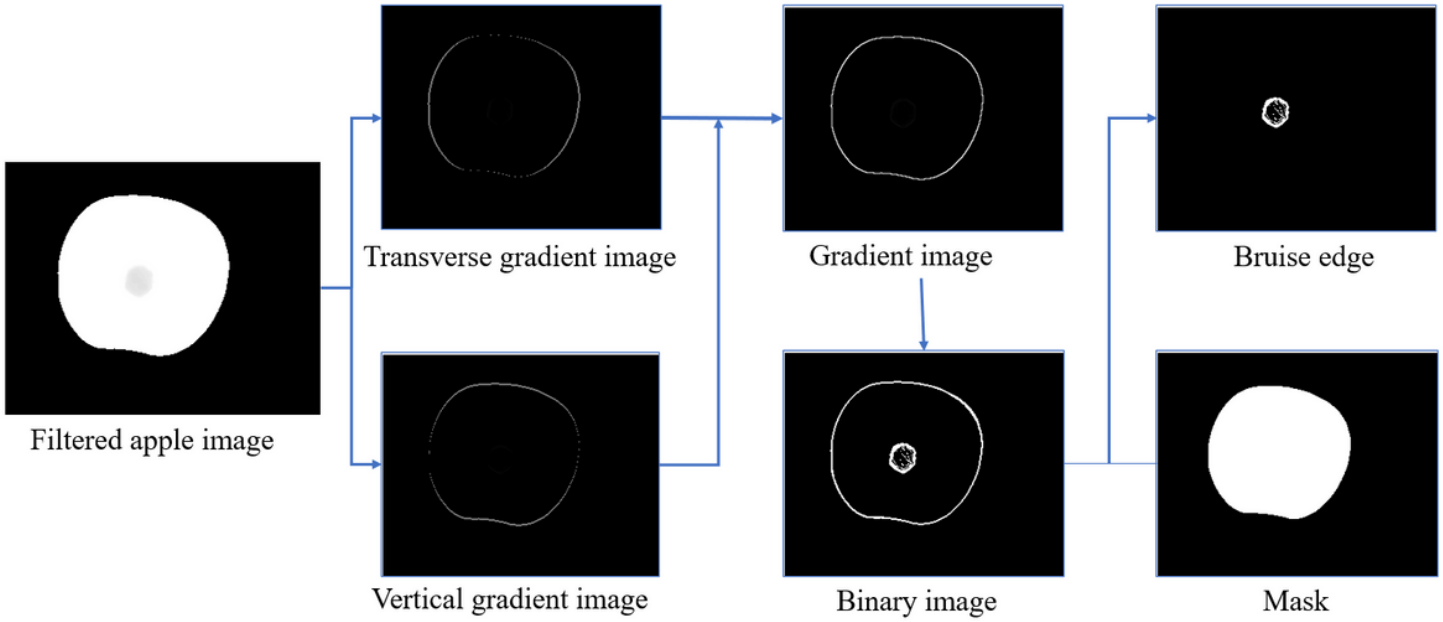

Figure 4

The bruise edge calculation for an apple sample

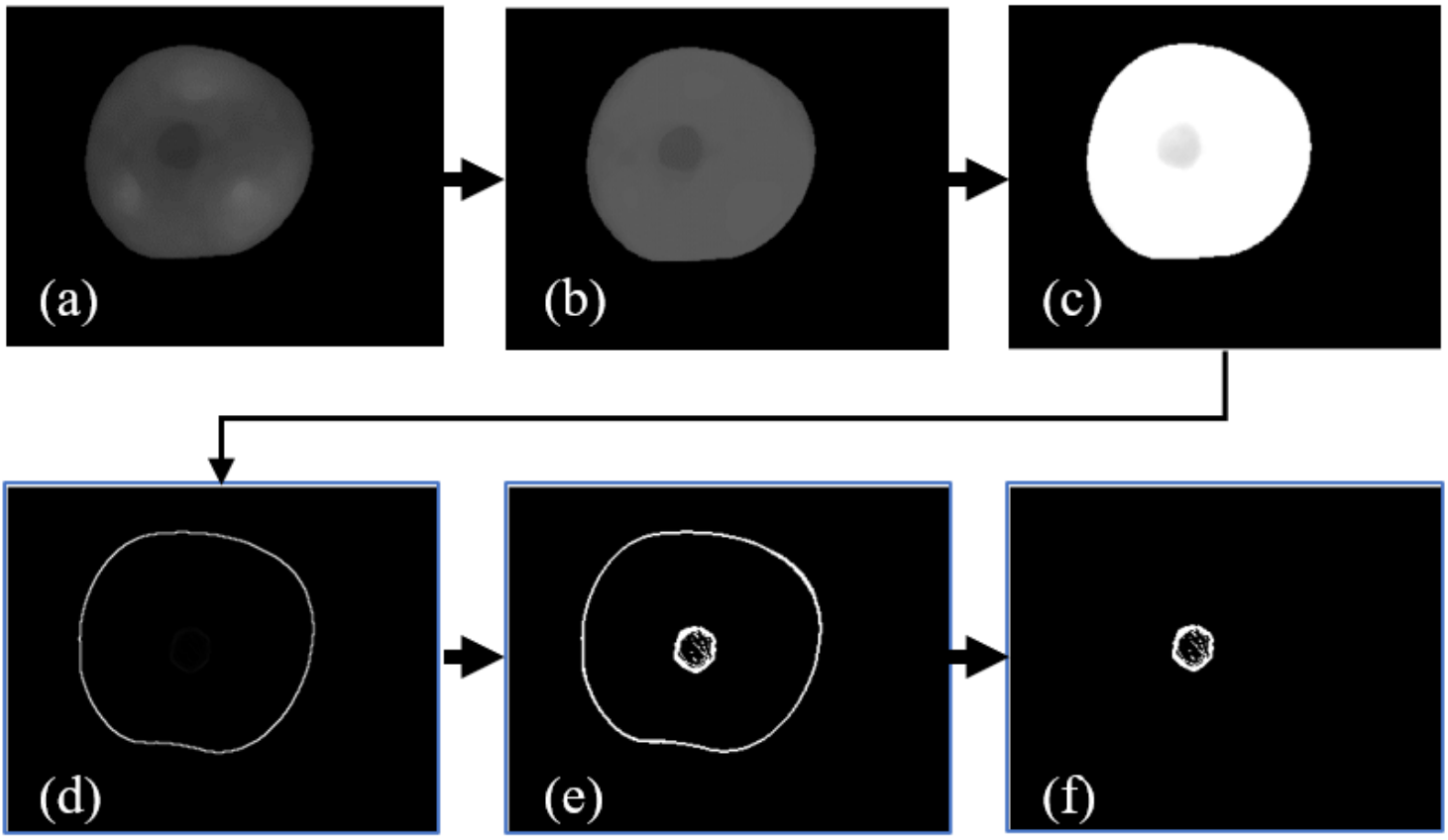

Figure 5

Two-level image preprocessing and image derivation for a bruised apple

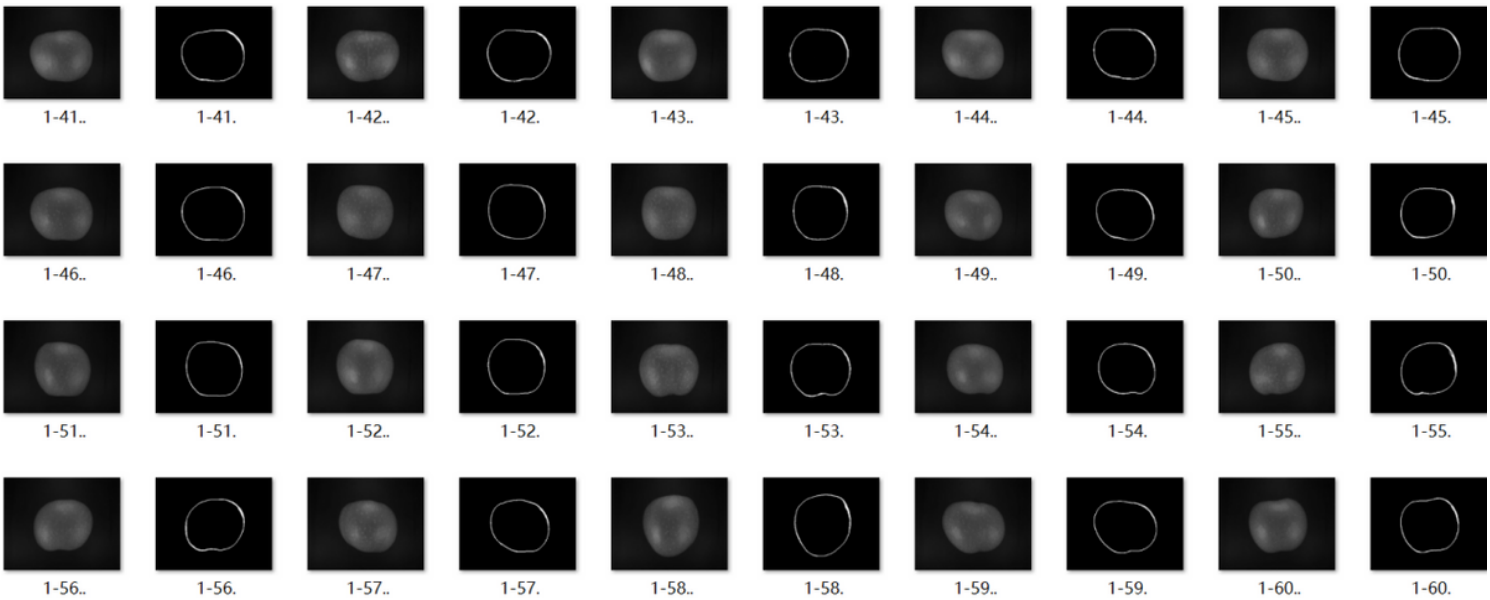

Figure 6

Identification results of 20 sound samples in the test set.

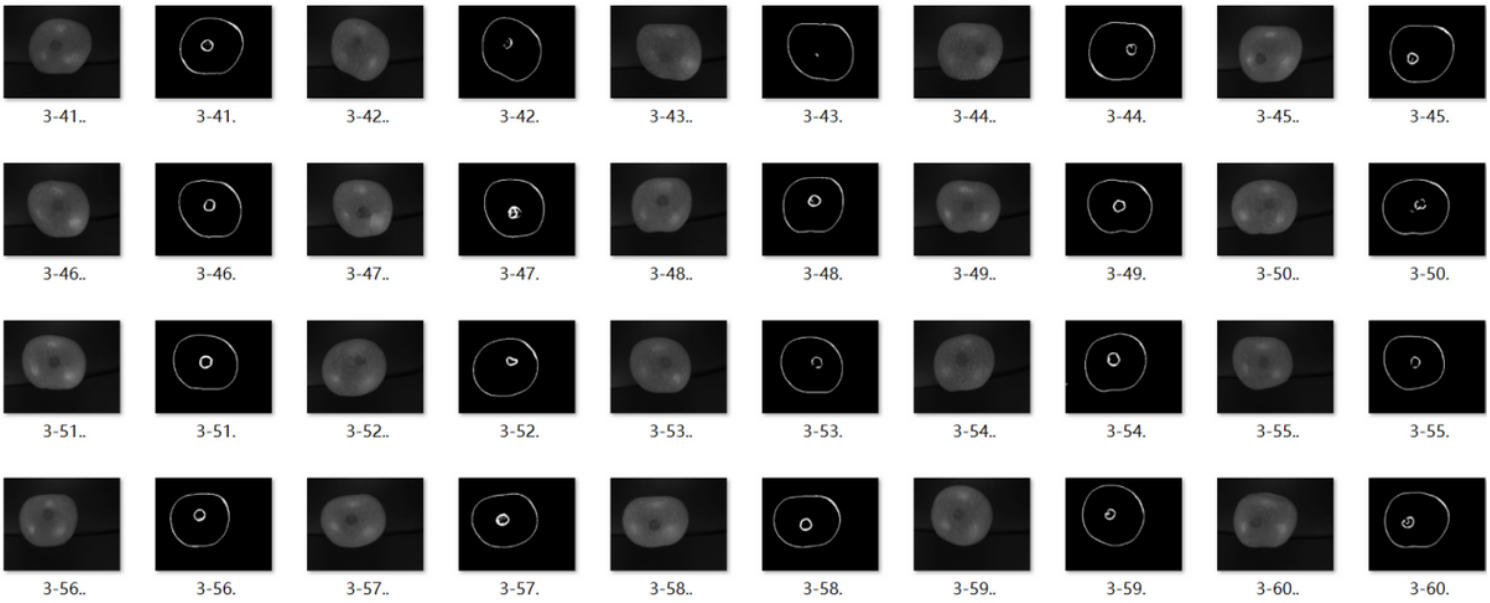

Figure 7

Identification results of bruised samples

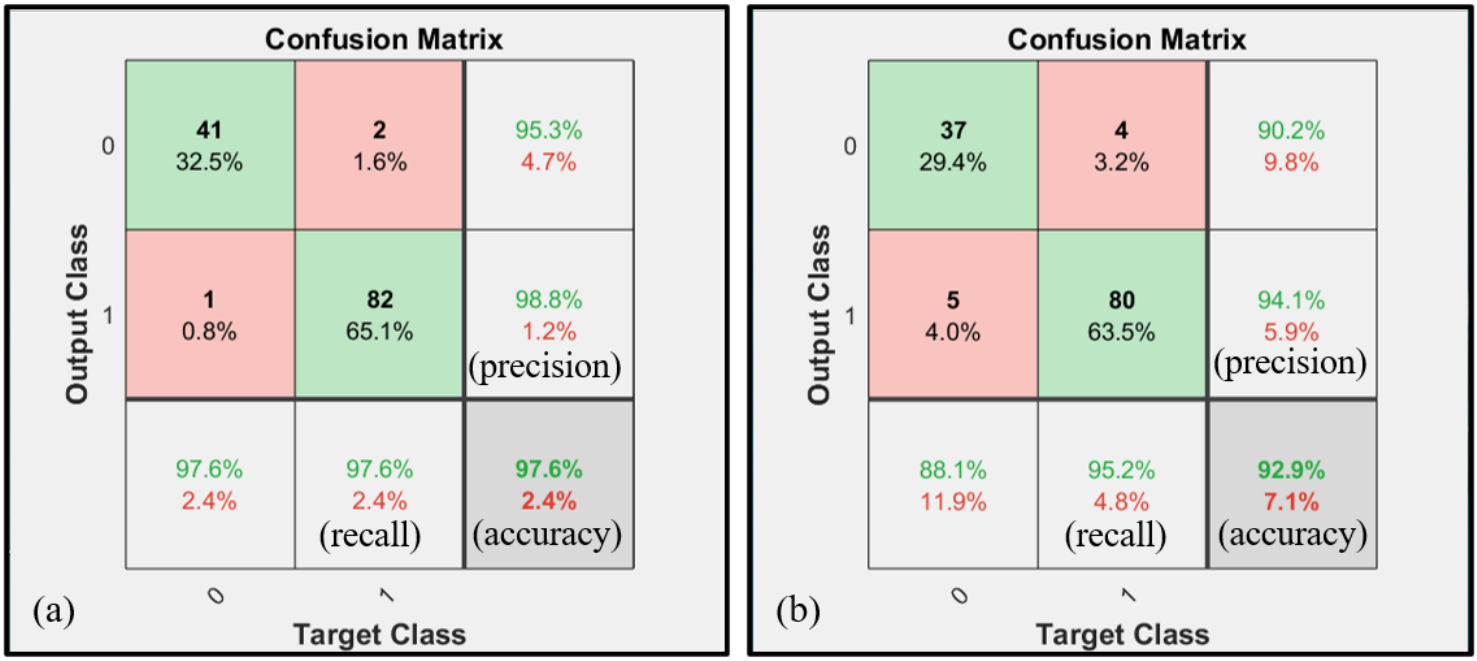

Figure 8

Confusion matrix